doi.org/10.36721/PJPS.2026.39.5.REG.14752.1

Cubosome-based nanoformulation of synthesized 1-cyclopentyl benzimidazole: *In-vitro* characterization and antibacterial evaluation

Tanzeela Masood[1], Ikram Ullah Khan[1], Sofia Hayat[2], Muhammad Irfan[1], Sajid Asghar[1], Umer Farooq[2], Muhammad Adnan Iqbal[2], Rabia Munir[1], Kai Bin liew[3], Khuriah Abdul Hamid[6,7], Sana Shahzad[4], Muhammad Saleem[5], Pervaiz Akhtar Shah[5], Nyla Ajaz[4] and Syed Haroon Khalid[1,6,7]*

[1]Department of Pharmaceutics, Faculty of Pharmaceutical Sciences, Government College University, Faisalabad, Pakistan
[2]Department of Chemistry, University of Agriculture, Faisalabad, Pakistan
[3]Faculty of Pharmacy, University of Cyberjaya, Persiaran Bestari, Cyberjaya, Selangor, Malaysia
[4]Department of Pharmacy, The University of Faisalabad, Faisalabad, Pakistan
[5]University College of Pharmacy, University of the Punjab, Lahore, Pakistan
[6]Faculty of Pharmacy, Universiti Teknologi Mara (UiTM), Cawangan Selangor, Kampus Puncak Alam, Bandar Puncak Alam, Selangor, Malaysia
[7]Innovative Drug Development and Delivery Research Group, Faculty of Pharmacy, Universiti Teknologi Mara, Cawangan Selangor, Kampus Puncak Alam, Bandar Puncak Alam, Selangor, Malaysia

Abstract: **Background**: Despite of having broad spectrum anti-bacterial activity, benzimidazole has limited clinical applications out of low solubility and bioavailability. Benzimidazole and cubosomal delivery systems are individually well studied, their combined application remains limited, particularly for newly designed derivatives with unexplored biological activity. **Objective**: This study reports the synthesis and characterization of *N*-cyclopentyl benzimidazole-loaded cubosomes for antibacterial application through improved solubility and controlled release. **Methods**: The *N*-cyclopentyl benzimidazole was synthesized by the reaction of benzimidazole with Bromo cyclopentane and confirmed by FT-IR, ^{1}H, and ^{13}C NMR spectroscopy. Cubosome nanoparticles were formed by the homogenization method, using glyceryl monooleate (GMO) as a lipid and poloxamer 407 (P407) as a surfactant. Different co-surfactants like Brij 35 (B 35), Myrj 52 (M 52), Tween 20 (T 20), and polyvinyl alcohol (PVA) as stabilizer were used to optimize the formulations and characterized for size, zeta potential, polydispersity index, entrapment efficiency, *in-vitro* drug release, and transmission electron microscopy. **Results**: Among the tested formulations, the cubosome containing 3% PVA demonstrated optimal characteristics, including a nanosize (~128 nm), high drug entrapment efficiency (94.08%), and colloidal stability. The antibacterial activity was assessed against *Staphylococcus aureus* and *Escherichia coli*. While the free drug exhibited larger zones of inhibition, the cubosome-encapsulated formulation showed sustained antibacterial effects, attributed to improved aqueous dispersion and prolonged release. **Conclusion**: These findings highlight the potential of cubosome-based delivery to enhance the solubility and therapeutic efficacy.

Keywords: Antibacterial activity; Cubosomes; 1-cyclopentyl benzimidazole; *In-vitro* characterization

Submitted on 17-06-2025 – Revised on 13-09-2025 – Accepted on 07-11-2025

INTRODUCTION

Lipid-based drug delivery systems have gained considerable attention due to their ability to encapsulate both hydrophilic and lipophilic drugs, alongside their biocompatibility, biodegradability and cost-effectiveness. As natural components of cellular structures and the human diet, lipids reduce cytotoxic risks compared to polymeric carriers (*Rapalli et al., 2021*). Lipid nanocarriers also enhance drug transport across skin, lymphatic, blood and brain barriers. Several delivery systems, such as liposomes, ethosomes, phytosomes, solid lipid nanoparticles (SLNs), nanostructured lipid carriers, and cubosomes, have been investigated, each offering distinct advantages and limitations (*Samimi et al., 2019*).

Among these, cubosomes are particularly attractive owing to their biocompatibility, bioadhesion, structural stability, and unique bicontinuous cubic phase morphology. Unlike SLNs and niosomes, cubosomes provide higher drug-loading capacity, sustained release, and improved bioavailability, making them especially suitable for poorly soluble antibacterial agents (Abourehab *et al*., 2020; *Yang and Marlin, 2020)*. Structurally, cubosomes are viscous, optically isotropic nanoparticles (10-500 nm) formed by self-assembly of amphiphilic lipids into a three-dimensional bilayer enclosing non-intersecting aqueous channels with an internal surface area of ~400 m^2/g (Tan *et al*., 2022). Their similarity to skin's bicontinuous architecture facilitates dermal retention and transport of drugs (Ali *et al.,* 2017). Moreover, their thermodynamic stability and versatility allow encapsulation of hydrophilic, lipophilic, and amphiphilic molecules, thereby improving solubility, protecting drugs from degradation, and enabling controlled release (Boge *et al*., 2019). Cubosome formation typically requires lipids such as glyceryl monooleate

**Corresponding author:* e-mail: syedharoonkhalid@gcuf.edu.pk

(GMO) or phytantriol combined with stabilizers like Pluronic® F127, which provides steric stabilization (Nakano *et al*., 2002).

Parallel to nanocarrier advances, heterocyclic compounds continue to be a cornerstone of drug discovery. Benzimidazole, a fused ring of benzene and imidazole containing two nitrogen heteroatoms, is a privileged scaffold in medicinal chemistry with diverse pharmacological properties *(Kamal et al., 2025),* notably antimicrobial activity (*Andrei et al., 2021*). Numerous benzimidazole derivatives have demonstrated potent antibacterial efficacy, even against resistant strains (*Alasmary et al., 2015*). They also serve as the basis for widely used anti-helminthic drugs such as albendazole, mebendazole, and flubendazole (*Tahlan et al., 2025*). Structure–activity relationship (SAR) studies highlight that substituents on the bicyclic ring strongly influence antibacterial activity (Goud *et al.,* 2019). Recent strategies have focused on N-alkylation at the N1-position to enhance lipophilicity (Ashraf *et al.,* 2025), membrane permeability and binding affinity, thereby improving antimicrobial potential (*Marinescu et al., 2020*).

Within this context, 1-cyclopentyl benzimidazole, synthesized via N-alkylation with bromocyclopentane, represents a promising antibacterial candidate (*Pathare and Bansode, 2021*). N-alkylated benzimidazoles have shown the ability to disrupt bacterial membranes and inhibit essential cellular processes (*Kumar et al., 2020*). However, despite the broad pharmacological applications of benzimidazoles, this specific analog has not been explored in advanced nanocarrier systems such as cubosomes.

Therefore, the present study aimed to develop cubosome-based nanoformulations of 1-cyclopentyl benzimidazole and evaluate their physicochemical characteristics (particle size, zeta potential, encapsulation efficiency and drug release) as well as antibacterial activity against *Staphylococcus aureus* and *Escherichia coli*. This work provides the first report of delivering 1-cyclopentyl benzimidazole via cubosomes, offering a potential strategy to enhance solubility, sustain release and overcome antimicrobial resistance.

MATERIALS AND METHODS

Materials

KOH, dimethyl sulfoxide (DMSO >99.5%), Bromocyclopentane, chloroform (99.8%), methanol (analytical grade), ethanol (analytical grade), Benzimidazole (analytical 99.9%), GMO (GRAS, 94%purity), poloxamer 407 (pharmaceutical grade, 99%), tween 20, PVA(polyvinyl alcohol), Brij 35, Myrj 52, hydrochloric acid, potassium monobasic phosphate and sodium hydroxide were got from Sigma Aldrich (St. Louis, USA). Distilled water used during experimentation was bought from the pharmacy in Faisalabad, Pakistan.

Synthesis of 1-cyclopentyl benzimidazole

The 1-cyclopentyl benzimidazole was synthesized according to the reported method with minor modifications (*Iqbal et al., 2015*). Benzimidazole (2 g, 0.0169 mol), KOH (1.5 eq, 1.42 g), and DMSO (40 mL) were added to a round-bottom flask and kept stirring for 30 minutes. Then alkyl halide (bromo-cyclopentane, 1 eq, 2.51 mL) was added dropwise with continuous stirring. The reaction takes place at RT with stirring continued for up to 3 h. After stirring, the reaction mixture was poured into 300 mL of cold water and placed for 2-3 h to let the mixture settle down. After that, the mixture was taken in a separating funnel, and the lower organic layer was extracted with chloroform. The extracted portion was kept at room temperature for the evaporation of chloroform to obtain the final product.

Characterization of 1-cyclopentyl benzimidazole

The solubility of the synthesized 1-cyclopentyl benzimidazole was checked in different polar and nonpolar solvents. The boiling point was calculated using the Gallen Kamp instrument (SANYO, JAPAN). FT-IR spectra were obtained using a Cary 630 spectrophotometer (Agilent Technologies, USA) equipped with an ATR module. Each sample was scanned in the range of 4000 to 650 cm^{-1} at room temperature. A total of 32 scans were recorded per sample with a resolution of 4 cm^{-1}. NMR analysis was conducted using a Bruker Avance 400 MHz spectrometer. The sample was dissolved in deuterium oxide (D_2O), and the spectra were recorded at ambient temperature. The chemical shifts for both ^{1}H and ^{13}C NMR were measured across ranges of 0–16 ppm and 0–220 ppm, respectively. Tetramethylsilane (TMS) was used as the internal standard. Proton peaks were characterized by their multiplicity, including singlets, doublets, triplets, and multiplets. UV–visible spectroscopic analysis of both benzimidazole compounds was carried out using methanol as the solvent. The spectra were recorded over a wavelength range of 200–800 nm to capture both ultraviolet and visible electronic transitions. Methanol was selected due to its good solvating ability and optical transparency in the studied range. High-performance liquid chromatography (HPLC) was employed to evaluate the chromatographic behavior and purity of the compound. The analysis was performed using a UV detector set at 230 nm, a wavelength commonly used for compounds exhibiting UV absorption. The retention time was recorded to assess the interaction of the compound with the stationary phase and its elution characteristics (*Nadeem et al., 2022*).

Development of cubosomes

Cubosomes were made using the previously described procedure, with a few modifications (*Al-Mahallawi et al., 2021*). The fifteen cubosomal dispersions (12 blank and 3

drug-loaded) were prepared using a homogenization method with different percentages of GMO, P407, PVA, T20, B35, M52. GMO was used as the lipid phase in a constant concentration of 3.5 % w/w, P407/T20/M52/B35 as the surfactants (1-3 % w/w) and PVA as an additional stabilizer (1.5 % w/w). The selection of process parameters such as homogenization speed (16,000 rpm), time (10 minutes) and temperature (60 °C) was based on preliminary screening experiments that ensured optimal dispersion and reproducibility of particle size. The choice of glyceryl monooleate (GMO) as the lipid matrix and poloxamer 407 (F-127) as the stabilizer was guided by their reported compatibility and ability to form a stable cubic phase structure. Different co-surfactants were screened to evaluate their impact on particle morphology, stability and drug entrapment efficiency. Each formulation was prepared and characterized in triplicate to ensure reproducibility and minimize batch-to-batch variation. The design approach was guided by comparative evaluation rather than a factorial design, which was considered appropriate for this preliminary optimization study.

The composition of formulations is shown in Table 1. GMO and P407 were kept on the hot plate for melting at 60 °C until they were fully homogenized and had a distinct appearance. Then, the temperature was raised to 100 °C and stirred at 1000 rpm. Secondly, aqueous phase containing PVA/B32/M 52/tween 20 was added to distilled water at the same temperature in a separate beaker. The GMO and P407 mixture was continuously stirred at 1000 rpm. Pre-heated aqueous phase containing co-surfactant was added dropwise into the GMO and P407 mixture until they were fully homogenized, and a milky white dispersion was produced. This dispersion was homogenized using (Heidolph, Silent Crusher M Homogenizer) at 16000 rpm for 10 minutes, hence it gave an opalescent appearance.

To produce drug-loaded cubosomes, API was added to the previously melted GMO and P407 mixture, while being continuously stirred at 1000 rpm. The rest of the procedure was the same as that adopted for blank formulation.

Characterization of cubosomes

FT-IR studies

The FT-IR spectra of the active pharmaceutical ingredient (API), excipients (GMO, POLOXAMER 407 and PVA) and the optimized drug-loaded cubosomal formulation were recorded using a Cary 630 FT-IR spectrophotometer (Agilent Technologies, USA) equipped with an attenuated total reflectance (ATR) accessory. Samples were directly placed on the ATR crystal without any additional preparation. Spectra were scanned over the range of 4000 to 650 cm^{-1} with a resolution of 4 cm^{-1} and each spectrum was obtained by averaging 32 scans. Background correction was performed before each measurement. The characteristic absorption bands observed were used to identify functional groups and assess potential interactions between the drug and excipients (Kapoor *et al*., 2020).

Measurement of pH and viscosity

Both the drug-loaded formulations and the blank formulations were measured for pH at 250 C using a portable pH meter (HI 9811-5 Hanna, Europe). Each formulation was used just enough to precisely dip the electrode, then it was stabilized for 5 minutes (Kapoor *et al*., 2020). The viscosity was measured by using a rotary viscometer (DVII, Brookfield, USA). The measurements were made at a shear rate of 20 rpm and a temperature of 25±0.5°C, using spindle # 2. Triplicate measurements were taken for each formulation to minimize the experimental uncertainties.

Particle size (PS), polydispersity index (PDI) and Zeta potential (ZP) measurement

The particle size (PS) and polydispersity index (PDI) of both blank and drug-loaded cubosome formulations were measured using a Malvern Zetasizer Nano ZS90 (Malvern Instruments, UK) equipped with dynamic light scattering (DLS) capability. Zeta potential (ZP) was determined via electrophoretic light scattering (ELS) using the same instrument, but only for drug-loaded formulations. Before measurement, all samples were diluted 1:100 with double-distilled water to minimize multiple scattering effects. Separate samples were prepared for PS and ZP analysis. All measurements were conducted at 25 ± 1 °C and dispersant parameters were set to standard values for water (viscosity: 0.8872 cP; refractive index: 1.330). Each experiment was performed in triplicate and the results are presented as mean ± standard deviation.

Transmission electron microscopy (TEM)

The morphological characteristics of cubosomes (P1, P2, P3) were examined using transmission electron microscopy (TEM, FEI Tecnai G2 Spirit BioTwin, USA). A drop of the diluted cubosome suspension was placed onto a carbon-coated copper grid and allowed to stand for 1-2 minutes (Ahmed *et al.,* 2024). Excess liquid was carefully wicked off using filter paper, and the grid was air-dried under ambient conditions. For contrast enhancement, negative staining was performed with 10% phosphotungstic acid (PTA). The samples were examined at an accelerating voltage of 120 kV and images were captured at various magnifications *(Nasr et al., 2015).*

Encapsulation efficiency

The centrifugation method was used to determine entrapment efficiency. A dispersion of cubosomes equivalent to 10 mg of drug was diluted with 9 mL of distilled water and transferred into centrifuge tubes. Samples were centrifuged at 6000 rpm for 30 minutes (*Karthika et al., 2018*). The amount of unentrapped drug present in the supernatant was quantified using a UV-Vis spectrophotometer (Cecil Instruments, Cambridge, England) at the predetermined λmax of 247 nm. Methanol was used only as a blank solvent for baseline correction. All measurements were performed in triplicate and entrapment efficiency was calculated accordingly. % EE was calculated through the following formula:

Table 1: Composition of blank and drug loaded formulations containing GMO, POLOXAMER 407 and different co-surfactants.

Formulations	GMO %	P407 %	PVA %	T 20 %	B 35 %	M 52 %	Drug %
Blanks							
F1	3.5	1.5	1	_	_	_	_
F2	3.5	1.5	2	_	_	_	_
F3	3.5	1.5	3	_	_	_	_
F4	3.5	1.5	_	1	_	_	_
F5	3.5	1.5	_	2	_	_	_
F6	3.5	1.5	_	3	_	_	_
F7	3.5	1.5	_	_	1	_	_
F8	3.5	1.5	_	_	2	_	_
F9	3.5	1.5	_	_	3	_	_
F10	3.5	1.5	_	_	_	1	_
F11	3.5	1.5	_	_	_	2	_
F12	3.5	1.5	_	_	_	3	_
Drug loaded							
P1	3.5	1.5	3	_	_	_	1
P2	3.5	1.5	3	_	_	_	2
P3	3.5	1.5	3	_	_	_	3

Glyceryl Monooleate (GMO); Poloxamer 407 (POLOXAMER 407); Polyvinyl Alcohol (PVA); Tween 20 (T 20); Brij 35 (B 35); Myrj 52 (M 52) and 1-Cyclopentyl Benzimidazole (Drug).

$$\% EE = \frac{\text{Total drug} - \text{Free drug}}{\text{Total drug}} \times 100$$

In-vitro drug release study

The release behavior of 1-cyclopentyl benzimidazole from cubosomal formulations was studied using a dialysis bag diffusion method. A cellulose membrane with a molecular weight cut-off (MWCO) of 12,000–14,000 Da was used. Before use, the membrane was soaked overnight in distilled water. After adding 1 mL of cubosome dispersion to the dialysis bag, the ends were securely sealed together using dialysis clamps and they were then immersed in 250 mL of 30% v/v ethanol in phosphate-buffered saline (pH 6.8) as the release medium and placed in the shaking water bath (Thermo Scientific-USA) at a maintained temperature of 37°C, 50 rpm (Gaballa *et al.,* 2020).

At intervals of 0, 0.5, 1, 2, 4, 6, 8, 12, and 24 hours, 5 mL of the medium was taken out and replaced with an equivalent volume of fresh dissolving medium. A phosphate buffer with a pH of 6.8 was used as a blank to measure the amount of medication released in the medium samples using UV-Vis spectroscopy at λmax 247 nm (*Hayat et al., 2025*). Each experiment was done in triplicate. The data was expressed as drug release from cubosomes at different time points**.** The cumulative amount of drug released was plotted over time and the release data were fitted to various kinetic models (zero-order, first-order, Higuchi and Korsmeyer-Peppas) to elucidate the drug release mechanism (*Prajapati,et al., 2014*).

Physical examination

All the formulated dispersions were analyzed for any physical modification that concerned appearance, phase separation, or any sort of precipitation. For this purpose, they were examined visually in proper lighting conditions and at RT.

Antibacterial activity of cubosomes

Antibacterial activity was evaluated using the agar well diffusion method by measuring the zone of inhibition. Nutrient agar was prepared and poured into sterile glass Petri dishes to form a uniform layer of approximately 4 mm thickness. After solidification, 1 mL of bacterial suspension standardized to 1.5×10^8 CFU/mL was evenly spread over the surface of each plate. The test organisms included *Escherichia coli* and *Staphylococcus aureus*. Excess inoculum was removed and the plates were allowed to stand at room temperature for 10 minutes to facilitate adherence of the microbial cells. Sterile wells of 10 mm diameter were created in the agar using a cork borer. Equal volumes of pure drug solution, the optimized cubosomal formulation (100 µg/mL) and a standard antibiotic disk (positive control) were introduced into separate wells. The plates were incubated at 37°C for 24 hours, after which the diameters of the inhibition zones surrounding each well were measured in millimeters. All experiments were conducted in triplicate and results were expressed as mean ± standard deviation (*Balouiri et al., 2016)*.

Stability study

The physical and chemical stability of selected cubosome formulations was evaluated over a period of 90 days at room temperature (25 ± 2 °C). Formulations were stored in airtight glass containers and sampled at predefined intervals (0, 30, 60 and 90 days) and evaluated for physical appearance, pH, viscosity, particle size, zeta potential and drug content. Drug content was determined using a validated UV-Visible spectrophotometric method at 247 nm (*Hayat et al., 2025*) and measurements were performed in triplicate.

Statistical analysis

Statistical analysis was carried out using two-way ANOVA to evaluate significant variations over time ($p < 0.05$ considered significant).

RESULTS

Synthesis of 1-cyclopentyl benzimidazole

The final synthesized product was obtained as a yellowish fluid and assessed by FT-IR and NMR spectroscopy. Yield: 92 %; B.P. 120 ℃. FT-IR (ATR, ν_{max}, cm^{-1}): 3054 (C-H_{arom}); 2955, 2871 (C-H_{aliph}); 1487, 1457, 1284, 1230 (C_{arom}-$N_{benzimi}$). ^{1}H NMR (500 MHz, D_2O, δ ppm): 0.79, 1.12, 2.62 (4 × CH_2), 3.61 (CH), 6.53 (NCHN), 7.27, 7.28, 7.33, 7.44 (Ar-H). ^{13}C NMR (125 MHz, D_2O, δ ppm): 25.6, 26.0, 34.14, 34.29 (4 × CH_2), 66.4 (CH), 113.04, 126.02, 124.14, 124.78, 135.8 (Ar-C), 143.71 (NCHN). Anal. Calcd for $C_{12}H_{14}N_2$; C, 77.38; H, 7.58; N, 15.04; found: C, 77.28; H, 7.49; N, 15.01.

Characterization of 1-cyclopentyl benzimidazole

The physical properties of the synthesized compound, 1-cyclopentyl benzimidazole, were measured, including solubility and melting point. The compound was obtained with a notable high yield, approximately 92 %. In terms of solubility, it demonstrated insolubility in the polar solvent water; however, it exhibited high solubility in polar organic solvents such as methanol, DMSO and dimethylformamide. For the evidence of the successful synthesis of 1-cyclopentyl benzimidazole, we noticed an intriguing FT-IR, in Fig. 1. The FT-IR spectrum of 1-cyclopentyl benzimidazole clearly showed the C-H_{arom} stretching vibration at 3054 cm^{-1} and the C-H_{aliph} vibration and C_{arom}-$N_{benzimi}$ stretching vibrations.

In the ^{1}H-NMR spectrum fig. 2, the aromatic proton peaks as multiplet were in the range of 7.27-7.44 ppm. An acidic proton peak of the NCNH group was present at 6.53 ppm as a singlet. The hydrogen peaks of the cyclopentyl group were observed at 3.61 ppm (-CH) and 0.79-2.62 ppm (-CH_2). In the ^{13}C-NMR spectrum fig. 2, the carbon signal of the NCHN group of *N*-alkylated benzimidazole was detected in the most downfield region at 143.71 δ ppm. The carbon peaks of the aromatic ring were detected at 113.04-135.8 δ ppm. The peaks of the cyclopentyl group carbon were observed at 66.40 ppm (-CH) and 25.67-34.29 ppm (-CH_2). Both compounds exhibited broad absorption bands in the ultraviolet region (200–350 nm) when recorded in methanol. A prominent wide absorption band was observed in the 250–350 nm region for each compound. In the visible region, additional absorption bands were detected for both compounds. Molecular orbital calculations indicated that these visible absorption bands correspond to electronic transitions between the highest occupied molecular orbital (HOMO) and the lowest unoccupied molecular orbital (LUMO). Frontier molecular orbital analysis showed that π atomic orbitals contribute predominantly to the HOMO and LUMO energy levels. As illustrated in fig. S1, the HOMO and LUMO orbitals are delocalized over the entire molecular framework. In contrast, the HOMO-1 orbital is mainly delocalized over the cyclopentyl group, while the LUMO+1 orbital is localized primarily on the benzimidazole moiety. The HPLC chromatogram displayed a single, sharp, and well-defined peak with a retention time of approximately 2.245 minutes, as shown in fig. S2. No additional peaks were observed within the chromatographic run. The observed peak exhibited a maximum height exceeding 500, indicating a relatively high concentration of the compound in the injected sample.

Selection of formulae for the preparation of cubosomes

The type and concentration of co-surfactant were varied systematically to assess their effects on particle size and dispersion uniformity. Formulations F1, F2, and F3 contained PVA 1, 2, and 3%, respectively, as co-surfactant. PVA is a synthetic polymer that was used as an additional stabilizer in the formation of cubosomes. Small particles with homogenous distribution are arranged by PVA. Formulations F4, F5, and F6 contain T 20 at 1, 2, and 3 %, respectively. T 20 is a nonionic surfactant with amphiphilic properties that reduces interfacial tensions and acts as the best co-surfactant when used with a combination of another surfactant. Formulations F7, F8 and F9 contain B 35 as 1, 2 and 3 % respectively.

Characterization of blank cubosomes formulations

All cubosomal dispersions were visually homogenized and milky colored, and there was no powder material deposited on the surface of the glass vial (ring formation). In addition, no macroscopic aggregates were present in any dispersion.

The pH of formulations varies from 5.9 to 6.9. The viscosity of the formulations varies from 0.88 to 2.01 cP. PS and PDI are shown in table 2. Formulation F1, F2, and F3 containing PVA showed particle sizes ranging from 133.9-72.49 nm. Formulations F4, F5, and F6 containing T 20 showed the PS ranging from 87.43-183.2 nm. PS of formulations F7, F8, and F9 containing B 35 showed the range of 233.2-175.5 nm. The formulation showed the size of the nano range and PDI of 0.6 to 0.5, indicating uniformity and homogeneity (Fig. 3). F10, F11 and F12, having M 52 as co-surfactant, had a size range of 118 - 215 nm and PDI of 0.5 to 0.3 After evaluating the PS and PDI of blank cubosome formulations, the F3 formulation was selected for subsequent drug loading. F3 formulation containing 3% PVA showed the best result based on the lowest PS and PDI of 72.49 nm and 0.2.

Optimization and characterization of drug-loaded formulations

The optimized formulation F3 (3% PVA) was identified based on comparative analysis of all developed batches. It demonstrated superior characteristics in terms of smaller particle size (72 nm) and narrow PDI (0.2), compared to other formulations.

Drug loaded cubosomes were prepared by adding up to 3 % of the drug to a mixture of GMO and POLOXAMER 407, followed by the addition of pre-heated water containing 3 % PVA. All drug-loaded formulations were within 121.01-155.5 nm size, as shown in fig. 3 and Table 2. As the ratio of the drug increased, the PS also increased. Formulation P1 has an average size of 121.01 nm, P2 has 154.1 nm containing 2 % of the drug and P3 has 155.5 nm containing 3 % drug. TEM images are presented in fig. 4, indicating that cubosomes are evenly distributed as separate particles. The nanocubic size depicted the smooth surface and consistency in the size range already determined by the Zetasizer.

The ZP of drug-loaded cubosomes showed the negative charges in table 2. The zeta potential values of the cubosomal formulations ranged from –17 to –22 mV.

Entrapment efficiency (% EE)

The % EE of the drug-loaded formulation was measured. As the amount of drug increased, the efficiency of entrapment also increased (Fig. 5). EE was found between 84.8 to 94.08%.

In-vitro drug release

Using the dialysis bag approach, *in-vitro* release study was conducted in PBS containing ethanol of pH 6.8 to assess the cubosomes' capacity to release the drug that was entrapped within them. A biphasic release pattern over a 24 h period was observed from cubosomes. The drug release profile curves are shown in fig. 6. It was revealed that among the three loaded formulations, the dispersion (P1) prepared with a 1 % w/w drug ratio exhibited a maximum release profile of 83.51%. Based on the *in-vitro* release studies, formulation P1 was selected for FT-IR and stability studies.

Fourier transform infrared spectroscopy.

The FT-IR spectra of API, PVA, GMO, POLOXAMER 407, and P1 cubosome formulation were studied to assess any possible interaction through the loss or shift of characteristic peaks shown in fig. 7. FT-IR spectra of API and excipients showed characteristic peaks without the appearance of new peaks.

Stability study

The stability investigations were conducted over three months at 25 °C and 75 % relative humidity to look for any changes in the final selected cubosomal formulation (P1) shown in Table 3.

Anti-bacterial activity

The antibacterial activity of pure drug and drug-loaded cubosomal formulations against *E. coli* and *S. aureus* was evaluated using the well-diffusion method. The zones of inhibition are shown in fig. 8 and summarized in Table 4. Among the cubosomal formulations, P3 showed the highest antibacterial activity.

DISCUSSION

The solubility characteristics and spectroscopic analyses (FT-IR and NMR) confirmed the successful synthesis of 1-cyclopentyl benzimidazole, in agreement with previously reported studies (*Chakraborty et al., 2018; Hayat et al., 2023*). The presence of characteristic C–H_arom, C–H_aliph, and C_arom–N_benzimidazole stretching vibrations in the FT-IR spectrum confirmed the integrity of the benzimidazole nucleus. Furthermore, the observed ^{1}H-NMR and ^{13}C-NMR chemical shifts validated N-alkylation without structural distortion (Mahmood *et al.,* 2025). These findings collectively confirm the chemical stability and purity of the synthesized compound, which is essential for reproducible formulation development.

Although the benzimidazole system contains lone pair electrons on the tertiary nitrogen atom, it is well established that $n \rightarrow \pi^*$ transitions are typically absent in benzimidazole derivatives (*Issa et al., 2006; Krishnamurthy et al., 1986; Mishra et al., 1985)*. Therefore, the broad absorption band observed in the 250–350 nm region can be confidently attributed to $\pi \rightarrow \pi^*$ transitions within the benzimidazole ring. The visible absorption bands arise from electronic transitions involving the frontier molecular orbitals. Molecular orbital analysis confirms that $\pi \rightarrow \pi^*$ transitions dominate the electronic excitation process, particularly transitions from HOMO-2, HOMO-1, and HOMO to the LUMO (Saral, *et al* 2017). The extensive delocalization of the HOMO and LUMO across the molecular skeleton facilitates these transitions, contributing to the observed absorption behavior. The localization of HOMO-1 on the cyclopentyl group and LUMO+1 on the benzimidazole ring further suggests that substituent effects and ring conjugation play a significant role in modulating the electronic properties of the compounds. Overall, the experimental UV–visible spectra are in good agreement with the theoretical molecular orbital calculations, confirming the nature of the observed electronic transitions. The HPLC chromatogram displayed a single, sharp, and well-defined peak with a retention time of approximately 2.245 minute**s** (Zamora *et al.,* 2009; Sun *et al.,* 2013; Ragno *et al.,* 2006). No additional peaks were observed within the chromatographic run. The observed peak exhibited a maximum height exceeding 500**,** indicating a relatively high concentration of the compound in the injected sample

The type and concentration of co-surfactants significantly influenced cubosome formation, particle size *(Cho et al., 2008*), and dispersion homogeneity, as previously reported (*Sanatkaran et al., 2014*). PVA-based formulations exhibited smaller particle sizes and lower PDI values, indicating superior steric stabilization and prevention of particle aggregation (*Kapoor et al., 2020*; *Kurangi, Jalalpure, & Jagwani, 2021)*. Increasing Tween 20

concentration resulted in particle size enlargement, which may be attributed to reduced interfacial tension leading to droplet coalescence and emulsion creaming (*Dickinson et al., 1999*). Brij 35 and Myrj 52 formulations demonstrated relatively larger particle sizes, possibly due to differences in hydrophilic–lipophilic balance and molecular packing behavior, consistent with earlier studies (*Ghosh & Moulik, 1998; Valizadeh et al., 2004*). The pH values of all cubosomal formulations ranged between 5.9 and 6.9, indicating compatibility with physiological and topical application requirements (*Verma et al., 2021*). The low viscosity values observed across formulations support enhanced spreadability and ease of administration *(Omar et al., 2019*). These physicochemical properties collectively suggest that the developed cubosomal systems are suitable for drug delivery applications without causing irritation or instability. Drug loading resulted in a noticeable increase in particle size, which may be attributed to the incorporation of drug molecules within the lipid bilayer and aqueous channels of the cubic phase (*Bei et al., 2009*). The increase in size was proportional to drug concentration, suggesting successful encapsulation within the cubosomal matrix. TEM analysis further confirmed the presence of uniformly distributed, discrete cubic nanoparticles with smooth surfaces, supporting the dynamic light scattering results and confirming structural integrity at the nanoscale. The zeta potential values of drug-loaded cubosomes ranged between −17 and −22 mV. Although these values were lower than the conventional ± 30 mV threshold for electrostatic stabilization, the presence of PVA provided effective steric stabilization, thereby preventing aggregation and maintaining dispersion stability (*Sherif et al., 2014; Salem et al., 2024*). A gradual decrease in zeta potential with increasing drug concentration may be attributed to surface charge shielding by encapsulated drug molecules (*Faisal et al., 2024*).

High entrapment efficiency observed across formulations can be attributed to the lipophilic nature of the drug and its strong affinity toward the lipidic cubic matrix of GMO (*Al-Sakini and Maraie, 2019*). The increase in entrapment efficiency with increasing drug concentration further suggests efficient accommodation of the drug within the internal structure of cubosomes (*Khan et al., 2018*). This high encapsulation efficiency is advantageous for reducing drug loss and improving therapeutic efficacy.

In-vitro drug release studies demonstrated a biphasic release pattern, characterized by an initial burst release followed by sustained drug release over 24 h, which is a typical behavior of cubosomal drug delivery systems (*Eldeeb et al., 2019; Jain et al., 2024*). The initial burst may be due to the release of surface-adsorbed drug, whereas the sustained phase reflects diffusion from the internal cubic structure. Formulation P1 showed higher cumulative drug release, which may be attributed to its smaller particle size and larger surface area (*Yadav et al., 2020*). In contrast, formulations with higher drug loading exhibited slower release profiles, likely due to stronger drug–lipid interactions and denser internal packing (*Garti et al., 2014*). FT-IR compatibility studies confirmed that no chemical interactions occurred between the drug and formulation excipients, as evidenced by the retention of characteristic peaks without the formation of new bands (*Patil et al., 2016; Almoudi et al., 2024*). This indicates that the drug was physically encapsulated within the cubosomal system, ensuring chemical stability and preserving pharmacological activity.

Stability studies conducted under accelerated conditions demonstrated no significant changes in particle size, zeta potential, or entrapment efficiency, confirming the robustness of the optimized formulation during storage. The stability of cubosomes may be attributed to the combined steric stabilization effect of PVA and the intrinsic thermodynamic stability of the cubic phase (*Salem et al., 2024*). The antibacterial activity studies showed that although the pure drug exhibited higher zones of inhibition, drug-loaded cubosomal formulations demonstrated sustained antibacterial activity. This behavior may be attributed to controlled drug release from the cubosomal matrix, resulting in prolonged exposure of bacterial cells to the drug. Among the formulations, P3 showed the highest antibacterial activity, possibly due to its higher drug content, which compensated for the sustained-release behavior. Similar findings have been reported for nano-based antimicrobial delivery systems (*Pourseif et al., 2023*).

CONCLUSION

This study aims to synthesize a chemical compound (1-cyclopentyl benzimidazole) of biological potential and encapsulate it into the cubosome formulation. The experimental design was justified through systematic screening of formulation components, validation of reproducibility and comparative performance assessment. Cubosomes were successfully prepared by the homogenization technique. The optimized cubosomal formulation (F3) presented sustained release effect, high entrapment efficiency and measurable anti-bacterial effect against *E. coli* and *S. aureus*. Although the free drug showed greater inhibition zones, the cubosome system demonstrated a controlled release profile that could potentially support prolonged therapeutic effects. The cubosomal formulation also addressed common formulation challenges associated with hydrophobic drug candidates, such as poor aqueous solubility. These findings suggest that cubosomes may serve as a promising carrier system for lipophilic drugs and warrant further investigation through *in-vivo* studies. Future studies will expand upon these results by including *in-vivo* validation and design-based optimization (e.g., factorial DOE) to further substantiate the robustness of the current findings.

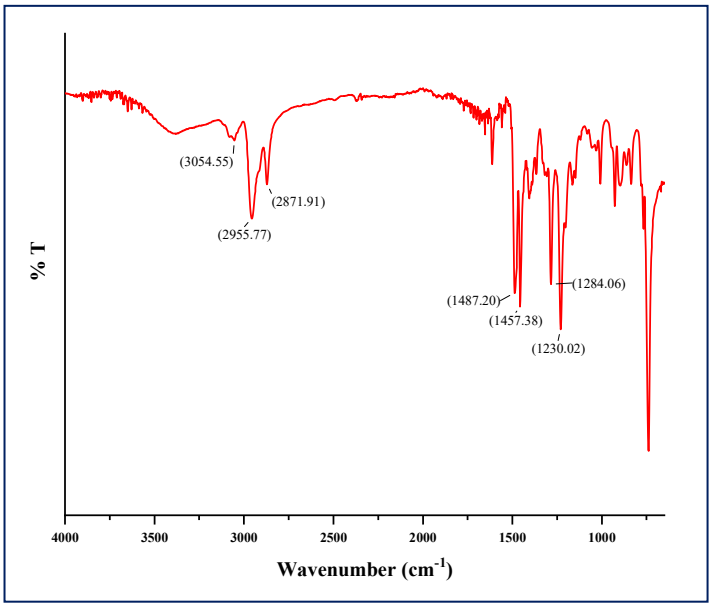

Fig. 1: FTIR spectrum of 1-Cyclopentyl benzimidazole, important absorbance peaks are labelled in the graph.

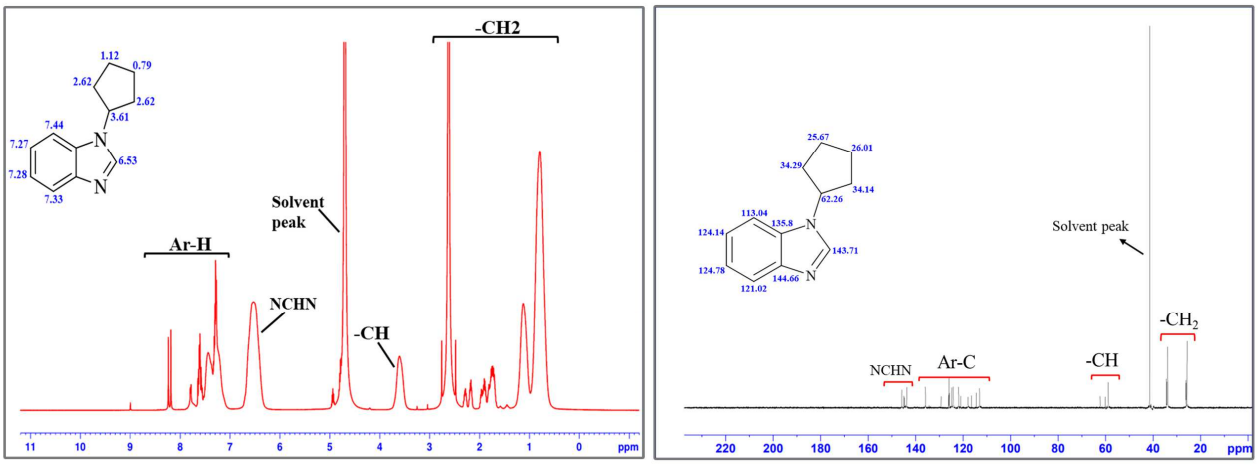

Fig. 2: ^{1}H (left)and ^{13}C (right)NMR spectrum of 1-Cyclopentyl benzimidazole.

Table 2: Particle size, polydispersity index, and zeta potential measurement of API loaded cubosomal formulations (P1-P3). Mean ± SD, N=3.

Formulations	PS (nm)	PDI	ZP (mV)
P1	121.01 ± 2.634	0.23 ± 0.026	-22.6 ± 1.069
P2	154.1 ± 2.665	0.146 ± 0.025	-18.5 ± 0.702
P3	155.5 ± 2.151	0.210 ± 0.030	-17.3 ± 1.792

Table 3: Stability data of pH, viscosity, drug content, PS, and ZP at RT for the P1 formulation. Mean ± SD, N=3.

Formulation	Days	pH	Viscosity (cP)	Drug content (%)	PS (nm)
P1	30	5.60 ± 0.002[a]	1.2 ± 0.004[b]	88.02 ± 1.43[c]	121.43 ± 1.216[d]
P1	60	5.45 ± 0.003	0.9 ± 0.003	89.32 ± 0.09	123.11 ± 2.118
P1	90	5.67 ± 0.002	1.1 ± 0.005	89.21 ± 1.24	123.86 ± 2.546

[abcde] indicates $p > 0.05$ vs. P1 at 30 and 60 days.

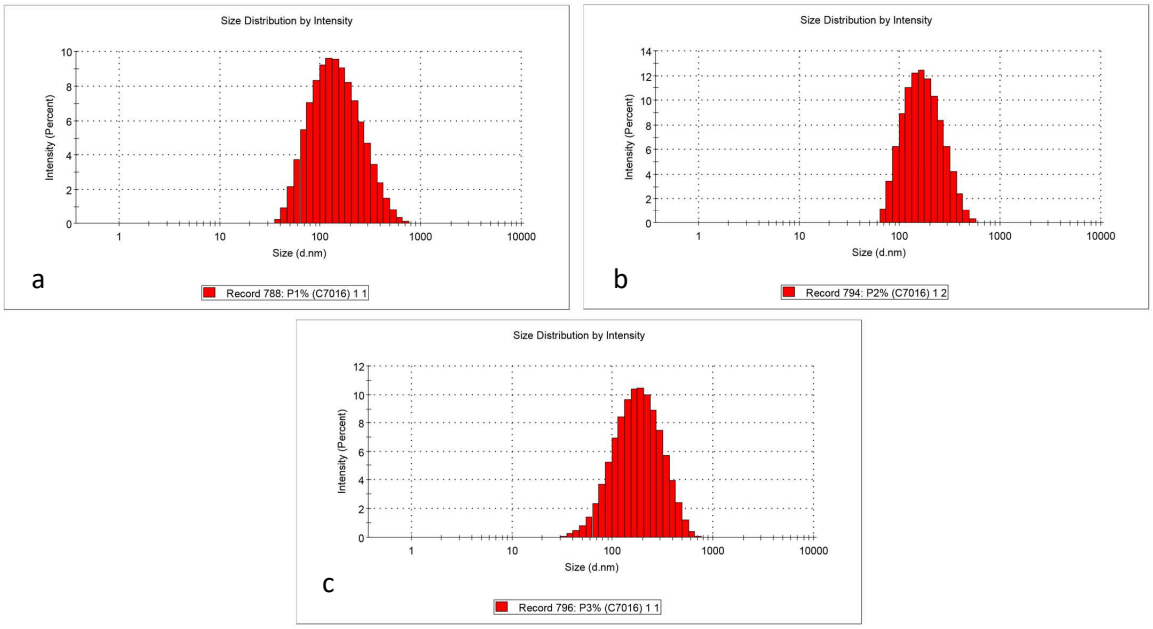

Fig. 3: Size distribution results of API loaded formulations (P1(a), P2(b) and P3(c)). Mean ± SD. N=3.

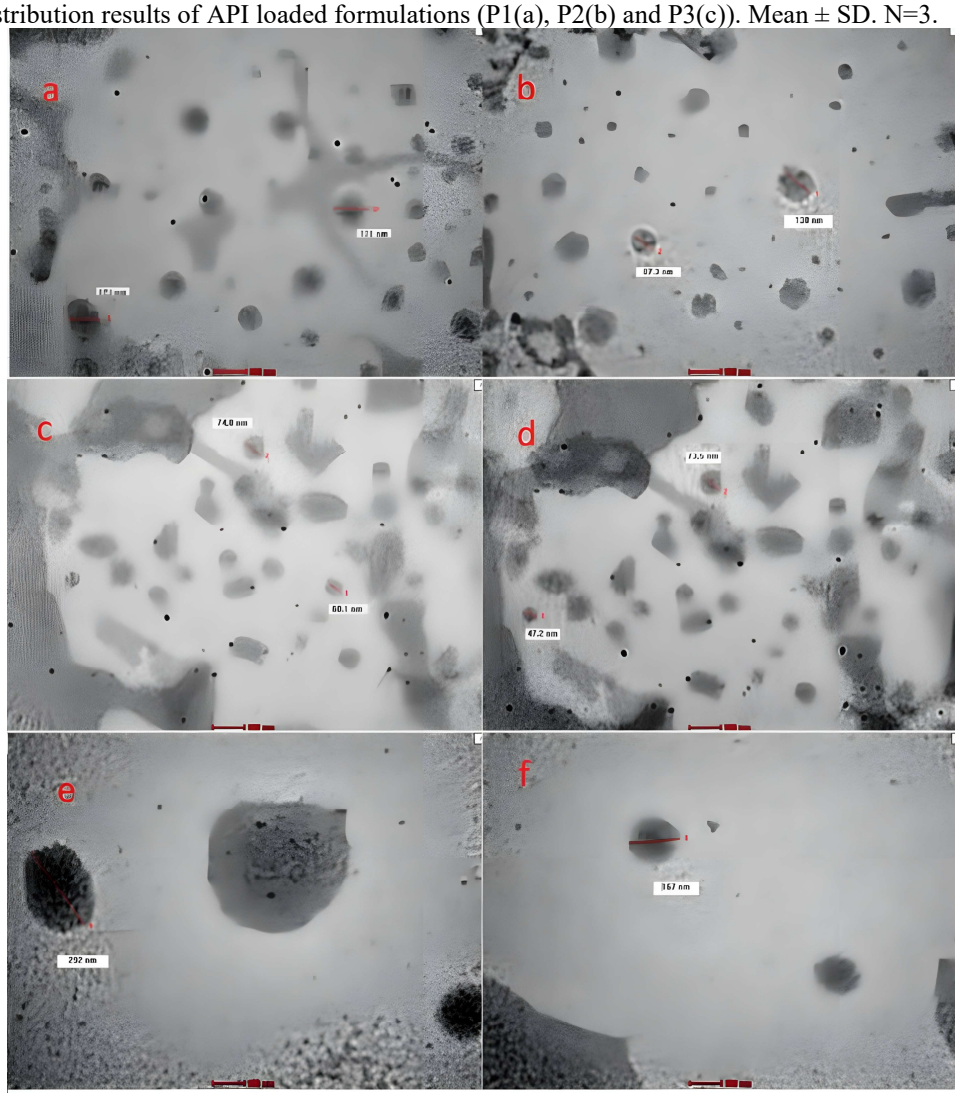

Fig. 4: TEM micrographs of P1 (a, b), P2 (c, d), and P3 (e, f) formulations.

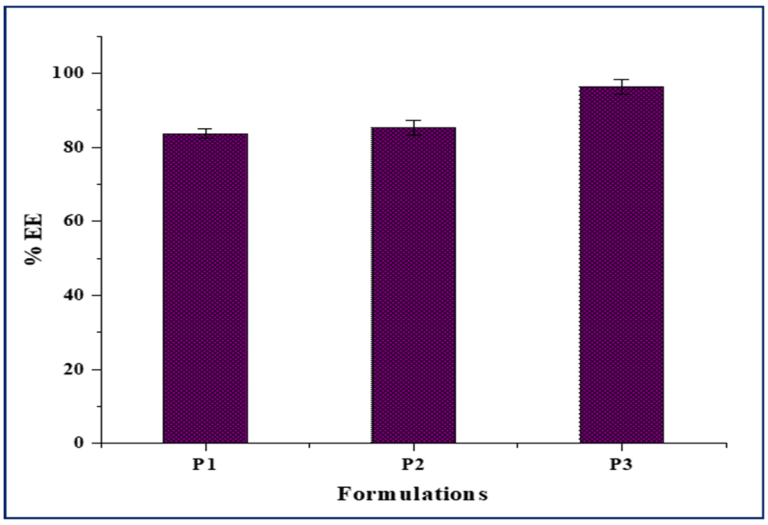

Fig. 5: % EE of API loaded formulations (P1-P3) is presented as Mean ± SD, n=3.

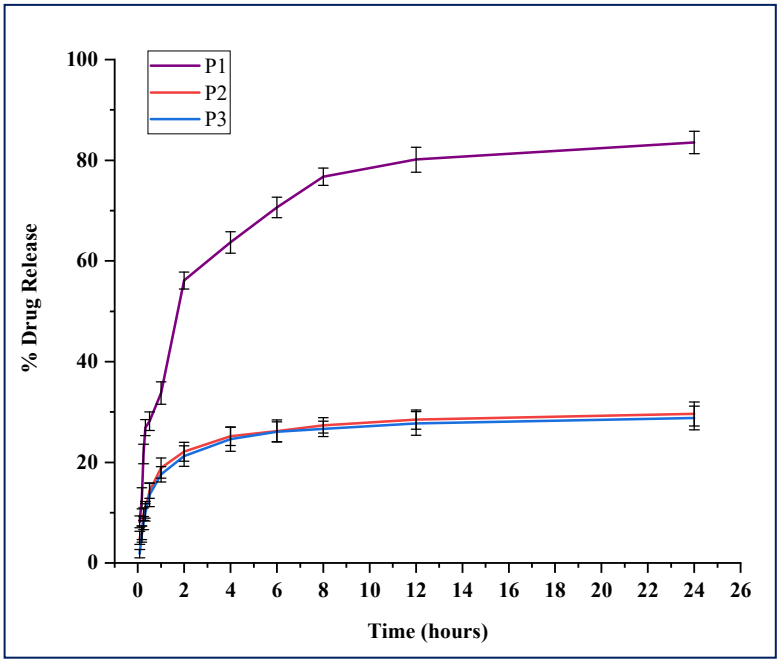

Fig. 6: *In-vitro* release profiles of API from cubosomal formulations P1, P2, and P3. Mean ± SD, n=3.

Table 4: The zone of inhibition of API (1-cyclopentyl benzimidazole) and drug loaded formulations against *S. aureus* and *E. coli* bacterial growth. Mean ±SD, N=3.

Formulations	Zone of Inhibition against *S. aureus*, size (mm)	Zone of inhibition against *E. coli*, size (mm)
P1	12 ± 0.2	10 ± 0.3
P2	13 ± 0.1	13 ± 0.3
P3	15 ± 0.5	16 ± 0.6
Pure drug (API)	28.9± 1.2	30.8 ± 0.8
Ciprofloxacin (Positive control)	24 ± 0.7	22 ± 0.4
Excipients without any drug (Negative control)	ND*	ND*

ND* = Not Detectable

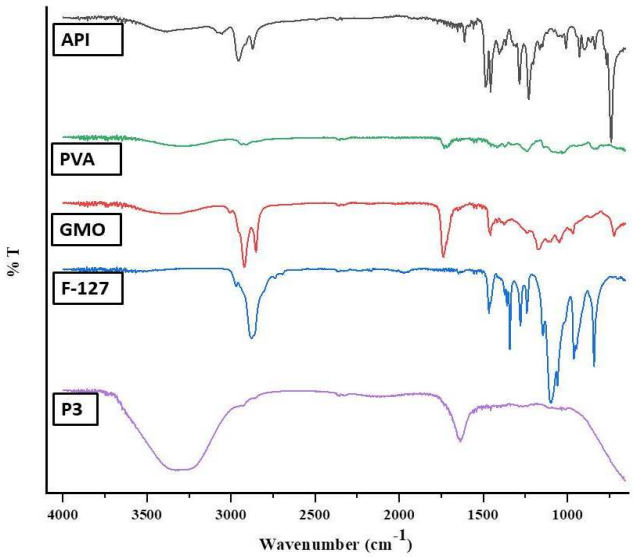

Fig. 7: FT-IR spectrum of API, PVA, GMO, POLOXAMER 407 and optimized cubosome dispersion (P3) showing the chemical compatibility of all excipients.

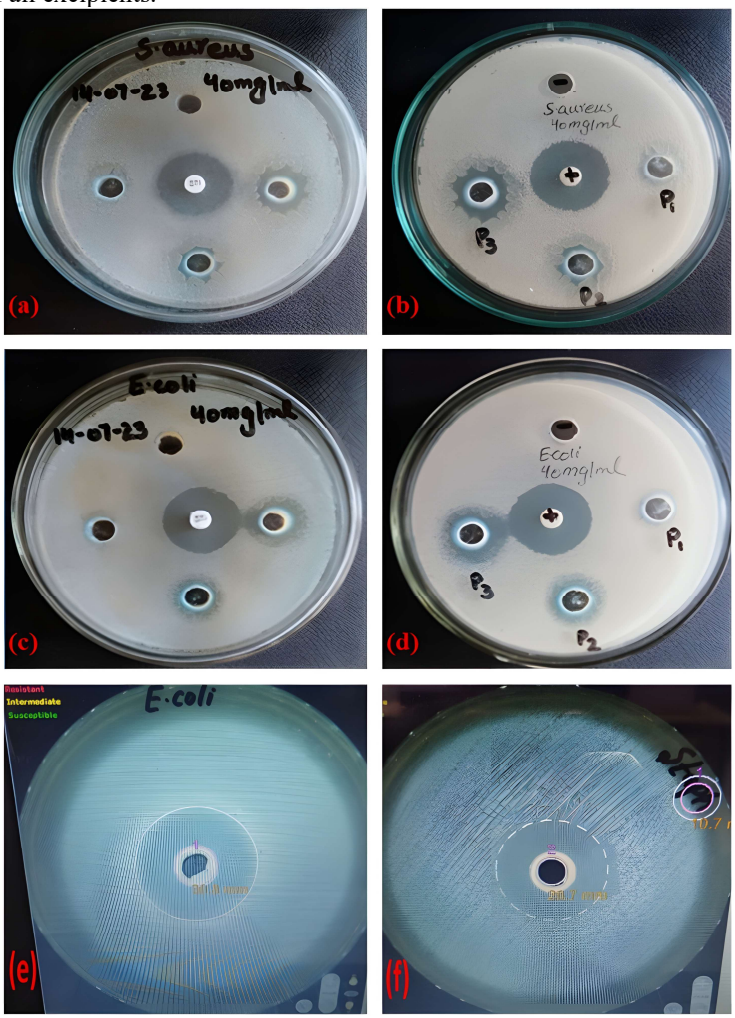

Fig. 8: Anti-bacterial activity of API (1-cyclopentyl benzimidazole) and drug-loaded formulations P1, P2, and P3 and positive control (ciprofloxacin) against *S. aureus* and *E. coli*. a (front) and b (back) show the zone of inhibition of the *S. aureus* strain. (c) and (d) show the zone of inhibition of the *E. coli* strain (front and back, respectively). (e) and (f) represent the activity of API.

Acknowledgments
The authors acknowledge the support provided by the Department of Pharmaceutics, Government College University, Faisalabad, Pakistan.

Authors' contributions
Tanzeela Masood: Methodology, software, validation, formal analysis, investigation, data curation and writing-original draft preparation; Ikram Ullah khan: Software and formal analysis; Sofia Hayat: Writing- review and editing; Muhammad Irfan: Data curation; Sajid Asghar: Formal analysis; Umer Farooq: Resources; Muhammad Adnan Iqbal: Resources, formal analysis and investigation; Rabia Munir: Validation, formal analysis and data curation; Kai Bin Liew: Resources; Khuriah Abdul Hamid: Resources and validation; Sana Shahzad: Data curation; Muhammad Saleem: Resources; Pervaiz Akhtar Shah: Validation; Nyla Ijaz: Resources; Syed Haroon Khalid: Conceptualization, writing-review and editing, visualization, supervision, project administration and funding acquisition.

Funding
There was no funding.

Data availability statement
The datasets generated during and/or analysed during the current study are available from the corresponding author on reasonable request.

Ethical approval
Ethical approval was not required for this study.

Conflicts of interest
No conflict of interest was declared by the authors.

Supplementary data
https://www.pjps.pk/uploads/2026/03/SUP1772957025.pdf

REFERENCES

Abourehab MA, Ansari MJ, Singh A, Hassan A, Abdelgawad MA, Shrivastav P, Abualsoud BM, Amaral LS and Pramanik S (2022). Cubosomes as an emerging platform for drug delivery: A review of the state of the art. *J. Mater. Chem. B.,* **10**(15): 2781-2819.

Ahmed MG, Gowda BH and Surya S (2024). Formulation and characteristic evaluation of tacrolimus cubosomal gel for vitiligo. *J. Dispersion Sci. Technol.,* **45**(2): 224

Alamoudi JA, Almoshari Y and Alotaibi HF (2024). Fabrication and evaluation of poloxamer facilitated, glyceryl monooleate based 5-fluorouracil cubosomes. *Ind. J. Pharm. Edu. Res.,* **58**(1): 91-98.

Alasmary FA, Snelling AM, Zain ME, Alafeefy AM, Awaad AS and Karodia N (2015). Synthesis and evaluation of selected benzimidazole derivatives as potential antimicrobial agents. *Molecules*., **20**(8): 15206-23.

Ali MA, Kataoka N, Ranneh AH, Iwao Y, Noguchi S, Oka T and Itai S (2017). Enhancing the solubility and oral bioavailability of poorly water-soluble drugs using monoolein cubosomes. *Chem. Pharm. Bull.*, **65**(1): 42-48.

Al-Mahallawi, Abdulaziz M, Abdelbary, Aly A, & El-Zahaby and Sally A (2021). Norfloxacin loaded nano-cubosomes for enhanced management of otitis externa: *In-vitro* and *in-vivo* evaluation. *Int. J. Pharmaceut*., **600**: 120490.

Al-Sakini SJ and Maraie NK (2019). *In-vitro* evaluation of the effect of using different gelling agents on the release of erythromycin from a nanocubosomal gel. *Al-Mustansiriyah J. Pharm. Sci.,* **19**(1): 34-43.

Andrei GŞ, Andrei BF and Roxana PR (2021). Imidazole derivatives and their antibacterial activity-a mini-review. *Mini Rev. Med. Chem.,* **21**(11): 1380-1392.

Ashraf R, Khalid Z, Qin QP, Iqbal MA, Taskin-Tok T, Bayil İ, Quah CK, Daud NAM, Alqahtany FZ, Amin MA and El-Bahy SM (2025). Synthesis of N-heterocyclic carbene-selenium complexes modulating apoptosis and autophagy in cancer cells: Probing the interactions with biomolecules and enzymes. *Bioorg Chem*, **160**: 108435.

Balouiri M, Sadiki M and Ibnsouda SK (2016). Methods for *in-vitro* evaluating antimicrobial activity: A review. *J. Pharm. Anal.,* **6**(2): 71-79.

Bei D, Marszalek J and Youan BB (2009). Formulation of dacarbazine-loaded cubosomes—part I: Influence of formulation variables. *AAPS. Pharm. Sci. Tech.,* **10**: 1032-1039.

Boge L, Hallstensson K, Ringstad L, Johansson J, Andersson T, Davoudi M, Larsson PT, Mahlapuu M, Hakansson J and Andersson M (2019). Cubosomes for topical delivery of the antimicrobial peptide LL-37. *Eur. J. Pharm. Biopharm.,* **134**: 60-67.

Chakraborty A, Debnath S, Ghosh T, Maiti DK and Majumdar S (2018). An efficient strategy for N-alkylation of benzimidazoles/imidazoles in SDS-aqueous basic medium and N-alkylation induced ring opening of benzimidazoles. *Tetrahedron.,* **74**(40): 5932-5941.

Cho YH, Kim S, Bae EK, Mok CK and Park J (2008). Formulation of a cosurfactant-free o/w microemulsion using nonionic surfactant mixtures. *J. Food Sci.*, **73**(3): E115-E121.

Dickinson E, Ritzoulis C and Povey MJ (1999). Stability of emulsions containing both sodium caseinate and Tween 20. *J. Colloid. Interf. Sci.,* **212**(2): 466-473.

Eldeeb AE, Salah S and Ghorab M (2019). Formulation and evaluation of cubosomes drug delivery system for treatment of glaucoma: Ex-vivo permeation and in-vivo pharmacodynamic study. *J. Drug. Deliv. Sci. Tec.,* **52**: 236-247.

Faisal MM, Gomaa E, Ibrahim AE, El Deeb S, Al-Harrasi A and Ibrahim TM (2024). Verapamil-loaded cubosomes for enhancing intranasal drug delivery:

development, characterization, ex vivo permeation, and brain biodistribution studies. *AAPS. Pharm. Sci. Tech.,* **25**(5): 95.

Gaballa SA, El Garhy OH, Moharram H and Abdelkader H (2020). Preparation and evaluation of cubosomes/ cubosomal gels for ocular delivery of beclomethasone dipropionate for management of uveitis. *Pharm. Res.*, **37**(10): 1

Garti N, Libster D and Aserin A (2014). Solubilization and delivery of drugs from GMO-based lyotropic liquid crystals. In: Nanoscience with liquid crystals: From self-organized nanostructures to applications., Cham: Springer International Publishing, pp.355-414.

Ghosh S and Moulik SP (1998). Interfacial and micellization behaviors of binary and ternary mixtures of amphiphiles (Tween-20, Brij-35, and sodium dodecyl sulfate) in aqueous medium. *J. Colloid. Interf. Sci.,* **208**(2): 357-366.

Goud NS, Ghouse SM, Vishnu J, Komal D, Talla V, Alvala R, Pranay J, Kumar J, Qureshi IA and Alvala M (2019). Synthesis of 1-benzyl-1H-benzimidazoles as galectin-1 mediated anticancer agents. *Bioorg. Chem.*, **89**: 103016.

Hayat K, Shkeel M, Iqbal MA, Khalid M, Quah CK, Wong QA, Rehman AU, Ahamed MB, Farooq U and Hameed S (2023). Inhibition of cell proliferation by azolium salts and silver (I)-N-heterocyclic carbene complexes: Synthesis, spectral and X-ray crystallographic characterizations. *Inorg. Chim. ACTA.,* **557**: 121694.

Hayat S, Farooq U, Nawaz M, Iqbal MA, Khalid SH, Nee TW, Masood T, Ahmad A, Ijaz MU and Fatima T (2025). Development of benzimidazolium salt-based cubosome hydrogel for topical treatment of burns. *J. Mol. Liq.*, **424**: 127048.

Issa RM, Hassanein AA, El-Mehasseb IM and El-Wadoud RIA (2006). UV–vis, IR and 1H NMR spectroscopic studies of some 6-chloro, 2-pyridyl hydrazones. *Spectrochim. Acta A Mol. Biomol. Spectrosc.*, **65**(1): 206-214.

Jain H, Prabhakar B and Shende PK (2024). Potentiation of brain bioavailability using thermoreversible cubosomal formulation. *Mol. Pharmaceut.,* **21**(5): 2534-2543.

Kamal A, Ibrahim AH, Al-Rawi SS, Iqbal MA and Bhatti, HN (2024). Biological potential of vinyl/allyl substituted imidazole-based N-heterocyclic carbene adducts: synthesis, spectral and X-ray crystallographic structural characteristics. *Chem. Pap.*, **78**(2): 851-860.

Kapoor KA, Pandit VI and Nagaich UP (2020). Development and characterization of sustained release methotrexate loaded cubosomes for topical delivery in rheumatoid arthritis. *Int. J. Appl. Pharm.,* **12**(3): 33-39.

Karthika VT, Sheri PS and Kuriachan MA (2018). Fabrication & evaluation of ketoprofen loaded cubogel for topical sustained delivery. *Int. J. Res. Rev.,* **5**: 149-159.

Khan S, Jain P, Jain S, Jain R, Bhargava S and Jain A (2018). Topical delivery of erythromycin through cubosomes for acne. *Pharma. Nanotech.*, **6**(1): 38-47.

Krishnamurthy M, Phaniraj P and Dogra SK (1986). Absorptiometric and fluorimetric study of solvent dependence and prototropism of benzimidazole homologues. *J. Chem. Soc., Perkin Trans.,* **2**(12):1917-1925.

Kumar A, Kumar Y, Sahu JK and Kumar S (2020). Synthesis, characterization and antimicrobial evaluation of some N-substituted benzimidazole derivatives. *Curr. Drug Discov. Technol.,* **17**(1): 87-91.

Kurangi Bhaskar, Jalalpure Sunil and Jagwani Satveer (2021). Formulation and evaluation of resveratrol loaded cubosomal nanoformulation for topical delivery. *Curr. Drug Deliv.,* **18**(5): 607-619.

Mahmood Z, Iqbal MA, Bhatti HN and Shahid M (2025). Alkyl-chain-wrenched lipophilic binuclear organoselenium compounds: Synthesis, characterization and evaluation of enhanced cytotoxicity. *Bioorg. Chem.*, p.108889.

Marinescu M, Cinteza LO, Marton GI, Chifiriuc MC, Popa M, Stanculescu I, Zalaru CM and Stavarache CE (2020). Synthesis, density functional theory study and *in-vitro* antimicrobial evaluation of new benzimidazole Mannich bases. *BMC Chemistry.,* **14**(1): 45.

Mishra AK and Dogra SK (1985). Photoluminescence of 2-(o-aminophenyl) benzimidazole. *J. Photochem.*, **31**(2-3): 333-344.

Nadeem RY, Yaqoob M, Yam W, Haque RA and Iqbal MA (2022). Synthesis, characterization and biological evaluation of Bis-benzimidazolium salts and their silver (I)-N-heterocyclic carbene complexes. *Med. Chem. Res*, **31**(10): 1783-1791.

Nakano M, Teshigawara T, Sugita A, Leesajakul W, Taniguchi A, Kamo T, Matsuoka H and Handa T (2002). Dispersions of liquid crystalline phases of the monoolein/oleic acid/Pluronic F127 system. *Langmuir.,* **18**(24): 9283-9288.

Nasr M, Ghorab MK and Abdelazem A (2015). *In vitro* and in vivo evaluation of cubosomes containing 5-fluorouracil for liver targeting. *Acta Pharmaceutica Sinica B*, **5**(1): 79-88.

Nazri MZ, Cilwyn B, Huda K, Sreenivasan S and Razali MR (2023). Synthesis, Structural and Anticancer Studies of Asymmetrical Dinuclear Silver (I) Di-N-heterocyclic Carbene Complexes. *Malaysian J. Chem.*, **25**(4): 207-221.

Omar S, Ismail A, Hassanin K and Hamdy S (2019). Formulation and evaluation of cubosomes as skin retentive system for topical delivery of clotrimazole. *J. Adv. Pharm. Res.,* **3**(2): 68-82.

Pathare B and Bansode T (2021). Biological active benzimidazole derivatives. *Results Chem.,* **3**: 100200.

Patil SS, Roy K, Choudhary B and Mahadik KR (2016). Fabrication of novel GMO/Eudragit E100

nanostructures for enhancing oral bioavailability of carvedilol. *Drug. Dev. Ind. Pharm.,* **42**(8): 1300-1307.

Pourseif T, Ghafelehbashi R, Abdihaji M, Radan N, Kaffash E, Heydari M, Naseroleslami M, Mousavi-Niri N, Akbarzadeh I and Ren Q (2023). Chitosan-based nanoniosome for potential wound healing applications: Synergy of controlled drug release and antibacterial activity. *Int. J. Biol. Macromol.,* **230**: 123185.

Prajapati V, Jain A, Jain R, Sahu S and Kohli DV (2014). Treatment of cutaneous candidiasis through fluconazole encapsulated cubosomes. *Drug Deliv. Transl. Re.,* **4**: 400-408.

Ragno G, Risoli A, Ioele G and De Luca M (2006). Photo- and thermal-stability studies on benzimidazole anthelmintics by HPLC and GC-MS. *Chem. Pharm. Bull.*, **54**(6): 802-806.

Rapalli VK, Banerjee S, Khan S, Jha PN, Gupta G, Dua K, Hasnain MS, Nayak AK, Dubey SK and Singhvi G (2021). QbD-driven formulation development and evaluation of topical hydrogel containing ketoconazole loaded cubosomes. *Mater. Sci. Eng. C,* **119**: 111548.

Salem EM, Dawaba HM, Abd Elbaset M, Gad S and Hassan TH (2024). Optimizing bioavailability and antihypertensive activity of Carvedilol cubosomes using D-optimal design: Comparative analysis of Cremophor RH 40 and Polyvinyl alcohol as secondary stabilizers. *J. Drug. Deliv. Sci. Tec.,* **97**: 105817.

Samimi S, Maghsoudnia N, Eftekhari RB and Dorkoosh F (2019). Lipid-based nanoparticles for drug delivery systems. In: Shyam SM, Shivendu R, Nandita D, Raghvendra KM, Sabu T (eds.), *Characterization and biology of nanomaterials for drug delivery*, Elsevier, UK, pp.47-76.

Sanatkaran N, Masalova I and Malkin AY (2014). Effect of surfactant on interfacial film and stability of highly concentrated emulsions stabilized by various binary surfactant mixtures. *Colloid Surface. A.,* **461**: 85-91.

Saral H, Ozdamar O and Ucar I (2017). Synthesis, structural and spectroscopic studies of two new benzimidazole derivatives: A comparative study. *J. Mol. Struct.,* **1130**: 46-54.

Sherif S, Bendas ER and Badawy S (2014). The clinical efficacy of cosmeceutical application of liquid crystalline nanostructured dispersions of alpha lipoic acid as anti-wrinkle. *Eur. J. Pharm. Biopharm.,* **86**(2): 251-259.

Sun M, Feng J, Luo C, Liu X and Jiang S (2013). Benzimidazole modified silica as a novel reversed-phase and anion-exchange mixed-mode stationary phase for HPLC. *Talanta*, **105**: 135-141.

Tahlan S, Singh S, Kaira M, Dey H and Pandey KC (2025). Benzimidazole-Based Anthelmintic Drugs: Synthetic Strategy, Pharmacological Insights, and SAR Analysis. *Chemistry Select*, **10**(10): e202405873.

Tan C, Hosseini SF and Jafari SM (2022). Cubosomes and hexosomes as novel nanocarriers for bioactive compounds. *J. Agr. Food. Chem.,* **70**(5): 1423-1437.

Valizadeh H, Nokhodchi A, Qarakhani N, Zakeri-Milani P, Azarmi S, Hassanzadeh D and Lobenberg R (2004). Physicochemical characterization of solid dispersions of indomethacin with PEG 6000, Myrj 52, lactose, sorbitol, dextrin, and Eudragit® E100. *Drug. Dev. Ind. Pharm.,* **30**(3): 303-317.

Verma Hk, Kumar V, Ain S, Kumar B and Ain Q (2021). Optimization and evaluation of developed topical ointment formulation containing cefadroxil and its antibacterial activity. *Int. J. of Pharm. Res., (09752366),* **13**(2): 3086-3096.

Yadav S, Sharma AK, Kumar P (2020). Nanoscale self-assembly for therapeutic delivery. *Front. Bioeng. Biotech*, **8**: 127.

Yang C and Merlin D (2020). Lipid-based drug delivery nanoplatforms for colorectal cancer therapy. *Nanomaterials*, **10**(7): 1424.

Zamora O, Paniagua EE, Cacho C, Vera-Avila LE and Perez-Conde C (2009). Determination of benzimidazole fungicides in water samples by on-line MISPE–HPLC. *Anal. Bioanal. Chem.,* **393**(6): 1745-1753.